SUPPLEMENTARY MATERIAL
Controlling the near-surface superfluid density in underdoped $YBa_2Cu_3O_{6+x}$ by photo-illumination

E. Stilp,[1,2] A. Suter,[1] T. Prokscha,[1] Z. Salman,[1] E. Morenzoni,[1] H. Keller,[2] P. Pahlke,[3,4] R. Hühne,[4] C. Bernhard,[5] J. C. Baglo,[6] Ruixing Liang,[6,7] W. N. Hardy,[6,7] D. A. Bonn,[6,7] and R. F. Kiefl[6]

[1] *Laboratory for Muon Spin Spectroscopy, Paul Scherrer Institut, CH-5232 Villigen PSI, Switzerland*
[2] *Physik-Institut der Universität Zürich, Winterthurerstrasse 190, CH-8057 Zürich, Switzerland*
[3] *Institut für Festkörperphysik, Technische Universität Dresden, D-01062 Dresden, Germany*
[4] *Institute for Metallic Materials, IFW Dresden, D-01069 Dresden, Germany*
[5] *Department of Physics, University of Fribourg, CH-1700 Fribourg, Switzerland*
[6] *Department of Physics and Astronomy, University of British Columbia, Vancouver, British Columbia, Canada V6T 1Z1*
[7] *Canadian Institute for Advanced Research, Toronto, Ontario, Canada M5G 1Z8*

(Dated: August 5, 2014)

Section S1: Photo illumination

The in-situ photo illumination was performed through a vacuum viewport using the "Bluepoint LED 400" from Hoenle [S1], mounted outside the ultra high vacuum (UHV) chamber (see Fig. 1). It is a spotlight consisting of four high intensity LEDs with a peak wavelength $\lambda_{\text{peak}} = 400(10)\,\text{nm}$ (corresponding to $E_\gamma = 3.1\,\text{eV}$). The output power in the focus is about $3.4\,\text{W/cm}^2$ at 80% intensity. To realize in-situ illumination, the focus had to be shifted from 1.5 cm to 2.2 m and the spot size had to be increased in order to match the sample size, with the use of two optical PCX lenses from Edmund Optics [S2] with focal lengths of $f_1 = 12\,\text{mm}$ and $f_2 = 305\,\text{mm}$. The resulting light spot on the sample position had a diameter of about 5 cm and an intensity of about $80\,\text{mW/cm}^2$. During the resistance measurements the sample was closer to the vacuum viewport and an intensity of about $200\,\text{mW/cm}^2$ was obtained. The temperatures and times for illumination and recovery of the samples during the μSR experiments are given in Table S I.

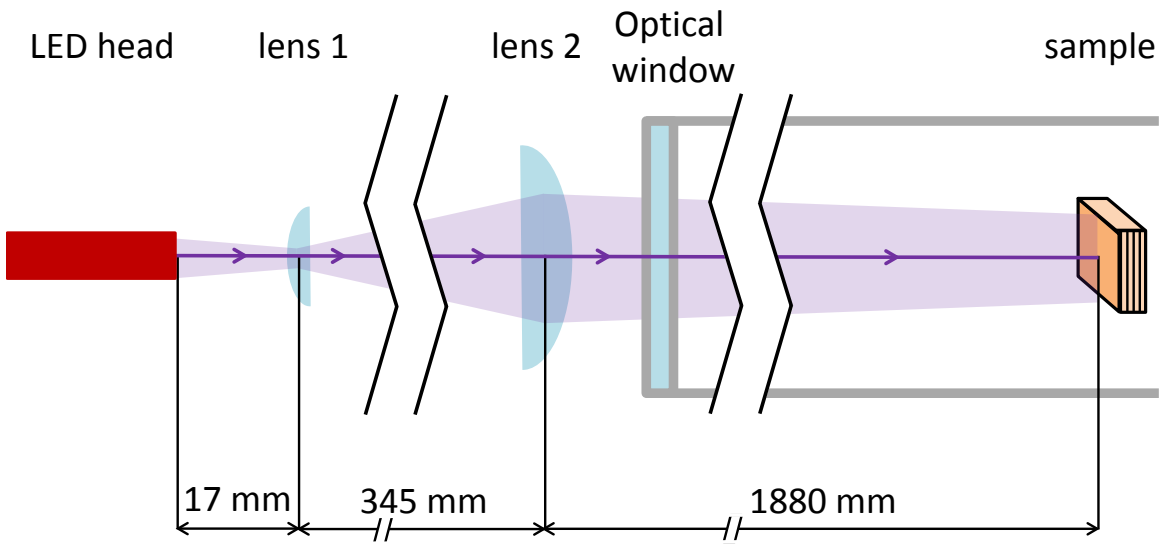

FIG. S 1: Schematic sketch of the illumination setup.

TABLE S I: Summary of the parameters used for the illumination and the recovery of the various YBCO samples during the LE-μSR experiments. The superconducting transition temperatures T_c were obtained from resistivity measurements for the thin films and with a Quantum Design MPMS SQUID magnetometer for the single crystals one year after the last annealing to set the oxygen content. The given values are averaged over the used samples. The uncertainty on $\overline{T_c}$ corresponds to the variation between the samples. The illumination temperature T_{illum}, illumination time t_{illum}, and the corresponding photon dose d_{ph} are listed. The given temperature T_{reset} and time t_{reset} have been used for the recovery.

Sample	$\overline{T_c}$	T_{illum}	t_{illum}	d_{ph}	T_{reset}	t_{reset}
$YBCO_{6.42}$ thin film	21(2) K	270 K	76 h	$4.4 \cdot 10^{22}$ photons/cm^2	315 K	24 h
$YBCO_{6.67}$ thin film	66.7(8) K	270 K	72 h	$4.2 \cdot 10^{22}$ photons/cm^2	315 K	16 h
$YBCO_{6.67}$ ortho-VIII	67.8(5) K					
for λ_a		270 K	80 h	$4.6 \cdot 10^{22}$ photons/cm^2	315 K	24 h
for λ_b		270 K	82 h	$4.8 \cdot 10^{22}$ photons/cm^2	310 K	24 h

Section S2: Ellipsometry measurements

The optical response of the YBCO thin-film samples in the spectral range near the 3.1 eV photon energy of the photo-doping was determined with ellipsometry. The measurements were performed at room temperature in air with a commercial spectroscopic ellipsometer (Woollam VASE [S3]) with a rotating analyser that covers the near-infrared to ultraviolet photon energy range of $0.5 - 6$ eV.

Ellipsometry is an optical technique in which the complex dielectric function of a material is obtained from the change of the polarization state of the light. Typically one uses linearly polarized light at a grazing angle of incidence and the information about the dielectric function is obtained from the analysis of the elliptically polarized reflected light. This elliptical polarization arises because the components with the polarization vector parallel (p) and perpendicular (s) to the plane of incidence experience a different attenuation and phase shift upon reflection at the ambient/sample interface. This effect is described by the Fresnel equations and is commonly expressed in terms of the ellipsometric angles Ψ and Δ, and the complex reflection coefficient $\tilde{\rho}$:

$$\tilde{\rho} = \frac{\tilde{r}_p}{\tilde{r}_s} = \tan(\Psi) \cdot e^{i\Delta},$$

where $\tilde{r}_p$ and $\tilde{r}_s$ are the reflection coefficients of the p- and s-component, respectively. For an optically isotropic material the complex dielectric function $\tilde{\epsilon}$ can be calculated from the relationship:

$$\tilde{\epsilon} = \epsilon_1 + i\,\epsilon_2 = \sin^2(\varphi) + \left(\frac{1-\tilde{\rho}}{1+\tilde{\rho}}\right)^2 \tan^2(\varphi)\ \sin^2(\varphi),$$

where φ is the angle of incidence of the light with respect to the surface normal ($\varphi = 0$ corresponds to the crystallographic c-axis).

In optically anisotropic materials, such as the cuprate high temperature superconductors, only the so-called pseudo-dielectric function $\langle\epsilon\rangle$ is obtained from the ellipsometry data. In many cases the ellipsometric response is still governed by the p-component and the pseudo-dielectric function is a good approximation to the component of the dielectric function parallel to the plane of incidence. The cuprates exhibit a fairly strong uniaxial anisotropy with a metal-like response along the direction of the CuO_2 planes (ab-plane), in contrast to an almost insulator-like behaviour in the perpendicular direction (along the c axis). For YBCO the optical anisotropy is fairly moderate in the optical and UV spectral range (of the interband transitions). A reasonable estimate of the dielectric function thus can be obtained from the as-measured pseudo-dielectric function. An accurate determination of the dielectric function still requires measurements at variable angles of incidence or on different surfaces for which the c axis is either parallel or perpendicular. The latter approach can be used for single crystals, while the former approach needs to be applied for epitaxial thin films for which the c axis is perpendicular to the surface. Therefore, we performed measurements at $\varphi = 35°, 50°$, and $80°$. The data have been analyzed with an optical model that contains a layer of a uniaxial material with independent dielectric function for the in-plane (ab-) and the out-of-plane (c-) directions and a semi-infinite STO substrate. The dielectric function of the latter is already known from independent measurements on a bare substrate. It should be noted that in the relevant energy range of 1 to 5 eV, the penetration depth of the light is significantly shorter than the film thickness. Thus, the optical response is governed by the YBCO film. The ellipsometric angles Ψ and Δ measured at the three angles of incidence were fitted simultaneously in a wavelength-by-wavelength manner by optimizing $\langle\epsilon_{ab}\rangle$ and $\langle\epsilon_c\rangle$. The penetration depth of the light, ζ, at normal incidence (for our photo-doping geometry

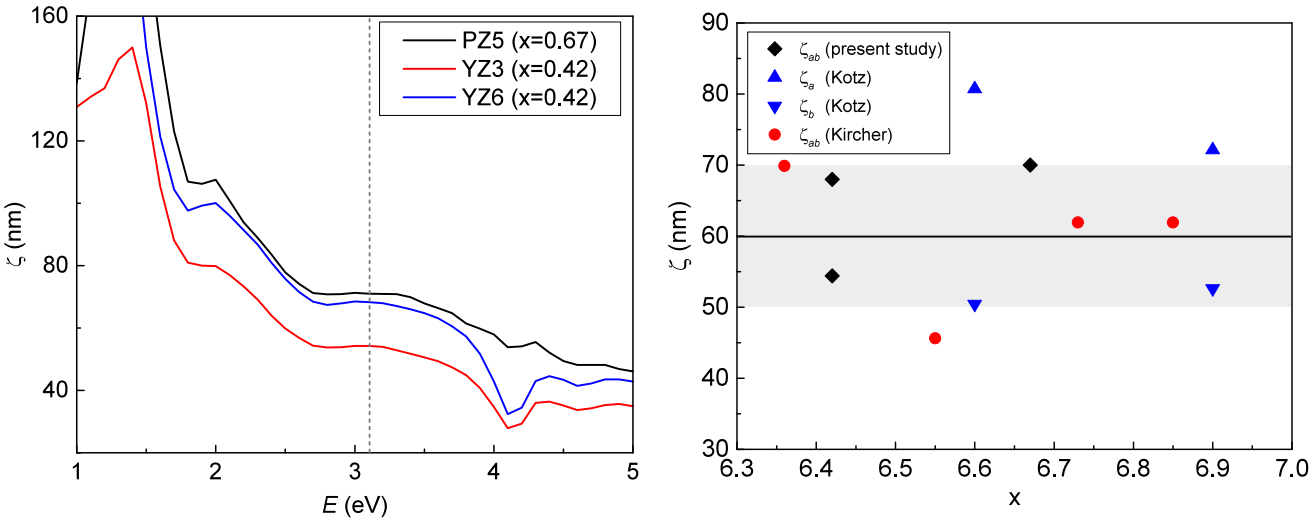

FIG. S 2: The determined penetration depth ζ versus the photon energy E for three YBCO thin film samples (left panel). The dashed line corresponds to the energy $E = 3.1\,\mathrm{eV}$, used for illumination in the μSR experiments. Overview of the penetration depth ζ for $E = 3.1\,\mathrm{eV}$ as function of doping x for YBCO samples of the present study and of the Refs. [S4, S5] (right panel). The indices i of ζ_i refer to the respective dielectric function ϵ_i. The black line and the grey area corresponds to the average light penetration depth and its error.

with $\varphi = 0°$) was calculated from the components of $\langle \epsilon_{ab} \rangle$ as follows:

$$\zeta = \frac{\lambda}{4\pi} \left(\frac{2}{\sqrt{\langle \epsilon_{1,ab} \rangle^2 + \langle \epsilon_{2,ab} \rangle^2} - \langle \epsilon_{1,ab} \rangle} \right)^{1/2} .$$

The value around 3.1 eV (equal to $\lambda = 400\,\mathrm{nm}$) that is relevant for our photo-doping experiment is in the range of $\zeta = 50 - 70\,\mathrm{nm}$ at both doping levels (see Fig. S 2) and agrees reasonably well with the estimates for YBCO single crystals of about $\zeta = 46 - 81\,\mathrm{nm}$ obtained from the data in Refs. [S4] and [S5]. Therefore we fixed ζ to 60 nm in the μSR data analysis.

Section S3: Magnetic penetration profiles in the Meissner state

For extreme type-II superconductors, where the coherence length is much smaller than the penetration depth, the screening of an applied magnetic field in the Meissner state ($H_{\mathrm{ext}} < H_{\mathrm{c_1}}$) is described by the London equation

$$\frac{\mathrm{d}^2 B(z)}{\mathrm{d}z^2} = \frac{1}{\lambda_{\mathrm{L}}^2} B(z) \propto n_s B(z) , \tag{S1}$$

where a constant superfluid density $n_s = n_{s_0}$ is assumed. The magnetic penetration depth λ_{L} is directly related to the superfluid density n_s:

$$\lambda_{\mathrm{L}}^2 = \frac{m^*}{\mu_0 \, e^2 \, n_{\mathrm{s}}},$$

where m^* is the effective mass of the supercarriers. For a semi-infinite sample the solution $B(z)$ is an exponential decay, whereas for thin films it is a superposition of two exponential decays from both surfaces. Due to the roughness of the surface [S6] and/or due to a reduction of the order parameter close to the surface, a dead layer of thickness z_0 is present at the interfaces. In this region the magnetic field is not screened. Then, the penetration profile of the initial state of the YBCO single crystals is described by:

$$B(z) = \begin{cases} B_{\mathrm{ext}} \, \exp\left[-(z - z_0)/\lambda_{\mathrm{L}}\right] & , z \geq z_0 \\ B_{\mathrm{ext}} & , z < z_0 \end{cases},$$

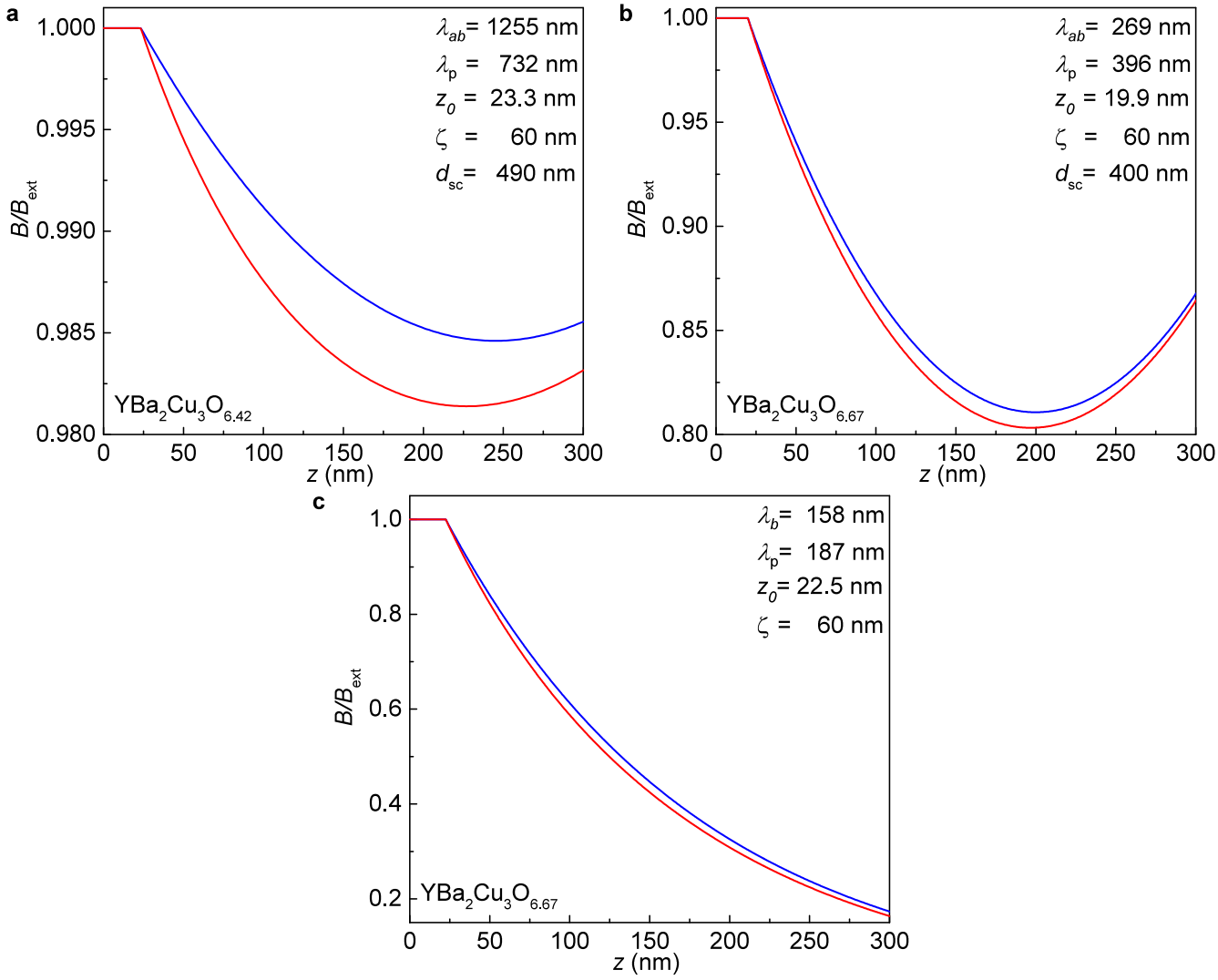

FIG. S 3: Calculated magnetic penetration profile $B(z)$ along the crystallographic c axis normalized to an applied magnetic field $B_{\rm ext}$ of thin-film $YBa_2Cu_3O_{6.42}$ (a), thin-film $YBa_2Cu_3O_{6.67}$ (b) and $YBa_2Cu_3O_{6.67}$ single crystals in the ortho-VIII phase (c). The presented field profiles correspond to the initial state (blue) and to the illuminated state (red). The parameters used for the fit are extracted from the μSR measurements.

where $H_{\rm ext} = B_{\rm ext}/\mu_0$ is the magnetic field applied parallel to the sample surface and z is the depth perpendicular to the surface (along the crystallographic c-axis for YBCO). For the YBCO thin films according to Eq. (S1) the Meissner screening is given as:

$$B\left(z\right) = \begin{cases} B_{\rm ext}\ \dfrac{\cosh\left[\left(z - z_0 - d_{\rm sc}/2\right)/\lambda_{\rm L}\right]}{\cosh\left[\left(d_{\rm sc}/2\right)/\lambda_{\rm L}\right]} & , z_0 \le z \le d_{\rm sc} + z_0 \\ B_{\rm ext} & , z < z_0, z > d_{\rm sc} + z_0 \end{cases}.$$

where $d_{\rm sc}$ is the thickness of the superconducting region.

These penetration profiles assume a constant superfluid density n_{s_0} as function of z. When YBCO is illuminated with visible light additional charge carriers are created. Our measurements show that the additional superfluid density is accumulated mainly at the vacuum interface, and therefore we modelled an exponential depth dependence of n_s according to the penetration of the light into the sample:

$$n_s = n_{s_0} + n_{s_p} \exp\left[-\left(z - z_0\right)/\zeta\right],$$

where ζ is of the order of the light penetration depth. Therefore, the London equation changes to:

$$\frac{\mathrm{d}^2 B\left(z\right)}{\mathrm{d}z^2} = \left\{ \frac{1}{\lambda_{\mathrm{L}}^2} + \frac{1}{\lambda_{\mathrm{p}}^2} \exp\left[-\left(z - z_0\right)/\zeta\right] \right\} B\left(z\right).$$

This equation can be solved analytically for the boundary conditions $B(z_0) = B(d_{\mathrm{sc}} + z_0) = B_{\mathrm{ext}}$. The solution for thin films in the range $z_0 \leq z \leq d_{\mathrm{sc}} + z_0$ is

$$\begin{aligned}\frac{B\left(z\right)}{B_{\mathrm{ext}}} = \frac{1}{N} \{ & I_{\nu_-}\left(\nu_{\mathrm{p}} \exp\left[-\left(z - z_0\right)/\left(2\zeta\right)\right]\right) \left[I_{\nu_+}(\nu_{\mathrm{p}}) - I_{\nu_+}(\nu_{\mathrm{p}}\beta)\right] \\ & - I_{\nu_+}\left(\nu_{\mathrm{p}} \exp\left[-\left(z - z_0\right)/\left(2\zeta\right)\right]\right) \left[I_{\nu_-}\left(\nu_{\mathrm{p}}\right) - I_{\nu_-}\left(\nu_{\mathrm{p}}\beta\right)\right] \},\end{aligned}$$

with

$$\begin{aligned} N &= I_{\nu_-}\left(\nu_{\mathrm{p}}\beta\right) I_{\nu_+}\left(\nu_{\mathrm{p}}\right) - I_{\nu_-}\left(\nu_{\mathrm{p}}\right) I_{\nu_+}\left(\nu_{\mathrm{p}}\beta\right), \\ \nu_{\pm} &= \pm\frac{2\zeta}{\lambda_{\mathrm{L}}}, \\ \nu_{\mathrm{p}} &= \frac{2\zeta}{\lambda_{\mathrm{p}}}, \\ \beta &= \exp\left[-d_{\mathrm{sc}}/\left(2\zeta\right)\right], \end{aligned}$$

where $I_\nu(z)$ is the modified Bessel function of the first kind [S7], which can be written as

$$I_\nu(z) = (z/2)^\nu \sum_{k=0}^{\infty} \frac{(z/2)^{2k}}{k!\,\Gamma\left(\nu + k + 1\right)}.$$

Since $\zeta \simeq 60\,\mathrm{nm}$ is short compared to $\lambda_{\mathrm{L}} \simeq 160/270/1260\,\mathrm{nm}$ (single crystal/thin film $x = 0.67$/thin film $x = 0.42$) the difference to the initial London model is a parallel shift at large z-values. Only at small z-values are the magnetic penetration profiles not parallel, and the magnetic field is screened more strongly. The penetration profile in the thin films becomes asymmetric and the minimum is shifted to lower z-values as shown in Fig. S 3a-b. These changes were observed in our μSR measurements.

For the single crystal, where a semi-infinite thickness is assumed ($d_{\mathrm{sc}} \to \infty$), the solution for $z > z_0$ is:

$$\frac{B\left(z\right)}{B_{\mathrm{ext}}} = \frac{I_{\nu_+}\left(\nu_{\mathrm{p}}\sqrt{\exp\left[-\left(z - z_0\right)/\zeta\right]}\right)}{I_{\nu_+}\left(\nu_{\mathrm{p}}\right)},$$

with

$$\begin{aligned} \nu_+ &= \frac{2\zeta}{\lambda_{\mathrm{L}}} \\ \nu_{\mathrm{p}} &= \frac{2\zeta}{\lambda_{\mathrm{p}}}. \end{aligned}$$

Here a stronger screening of the applied magnetic field is also observed for small z-values, whereas a parallel shift to smaller $B(z)$-values is observed for larger z-values as depicted in Fig. S 3c.

Using this model the parameter listed in Tab. II have been obtained for the investigated sample sets.

TABLE S II: The London penetration depth λ_{L} and the dead layer to the vacuum interface z_0 determined with a global fit of the LE-μSR spectra for YBCO in the initial state. The photo-induced penetration depth λ_{P} extracted from LE-μSR spectra of the illuminated state.

Sample		z_0	λ_{L}	λ_{P}
$YBCO_{6.42}$ thin film		23(2) nm	1255(10) nm	732(20) nm
$YBCO_{6.67}$ thin film		19.9(3) nm	269(1) nm	396(5) nm
$YBCO_{6.67}$ ortho-VIII	B||b-axis	24.4(9) nm	177(5) nm	-
	B||a-axis	22.5(7) nm	158(2) nm	187(12) nm

[S1] http://www.hoenle.de/uv-produkte/uv-geraete-bluepoint/bluepoint-led/
[S2] http://www.edmundoptics.com/optics/optical-lenses/plano-convex-pcx-spherical-singlet-lenses/laser-grade-plano-convex-pcx-lenses/3212
[S3] http://www.jawoollam.com/vase_home.html
[S4] J. Kircher et al., Phys. Rev. B **44**, 217-224(1991).
[S5] A. L. Kotz et al., Phys. Rev. B **45**, 2577-2580(1992).
[S6] M. Lindstrom, B. Wetton, and R. Kiefl, J. Eng. Math., DOI 10.1007/s10665-013-9640-y.
[S7] M. Abramowitz and I. A. Stegun, *Handbook of Mathematical Functions with Formulas, Graphs, and Mathematical Tables* (U.S. Government Printing Office, Washington, 1972)